

Surface Correction Control Based on Plasticized Multilayer P(VDF-TrFE-CFE) Actuator—Live Mirror

Kritsadi Thetpraphi, Minh Quyen Le, Afef Houachtia, Pierre-Jean Cottinet, Lionel Petit, David Audigier, Jeff Kuhn, Gil Moretto, and Jean-Fabien Capsal*

The interdisciplinary approach presented here creates next-generation large mirrors using electroactive polymer (EAP) actuators without classical glass abrasive polishing (“live mirrors”). The outstanding electromechanical coupling properties of terpolymer are taken advantage of, particularly when doped with plasticizer, e.g., diisononyl phthalate (DINP). This doped terpolymer creates a large strain response as well as excellent mechanical energy density under relatively low electric fields. Classical EAPs (e.g., polyurethane, silicone) require extremely high input voltages to reach sufficient mechanical strain. Using the high-permittivity doped terpolymer and the concept of stacking multilayers, high displacements and large forces are generated. The actuation performance of multilayered terpolymer filled with DINP has been proven to shape mirror glass with a preliminary prototype of an 8-layer actuator stack. The experimental results demonstrate surface deformations under load conditions of several microns. This is large enough to usefully control large optical telescope mirrors. This technology may enable much larger high-quality optical mirror systems for ground- and space-based astronomy and communications telescopes.

1. Introduction

Optical communication and remote sensing, including astronomy, are currently limited by the cost and manufacturability of their high-quality large optics. Innovations that decrease the cost or allow larger mirrors may greatly improve

high-bandwidth communication, civil space surveillance technologies, wireless optical communication systems (UV and free-space systems), hyper-aperture multi-mirror structures, geoengineering (space mirror), and astronomical systems.^[1,2] In particular the light-gathering power of an optical telescope, its “light grasp” or aperture gain, is one of the most important features of a telescope,^[3] which requires very precise glass mirror technology.

Recently, we have proposed a “World’s Largest Telescope” for achieving high-contrast observations that could use this technology.^[4–6] Such an optical system will be limited by the cost and manufacturability of large mirrors. The work described here, optics fabricated from an optimized electroactive polymer (EAP), could enable optics like these. The new approach will extend conventional active mirror technologies to larger smooth optical surfaces, without abrasive polishing. This means it will be possible to create precisely shaped

low scattered light mirrors—suitable to astronomical applications—faster and at lower production costs. Our long-term vision for the new technology is to decrease the mass density (and cost) of mirrors by an order of magnitude.

The idea of using force actuator-sensors fabricated from EAPs^[3,4] is developed in this work in order to achieve active mirror surface shape control. By manipulating EAPs as active supports, integrated into the mirror structure allows correcting the mirror shape with a continuous actuator force distribution. **Figure 1** illustrates how EAPs behave as elastic electromechanical deforming springs. This “electrical polishing” can correct surface shape errors that would be conventionally removed by abrasive grinding. To achieve high optical mirror quality surfaces with a thickness of a few millimeters the EAP glass deformation must have a dynamic range of few microns corresponding to actuator forces of about 1 N. The technique we propose could potentially be achieved using only additive manufacturing via 3D-printing technology.

In this article we aim to present the EAP concept for Live-Mirror active optics. We evaluate different polymers in specific actuator designs in order to test their mechanical actuation properties for mirror-actuator prototypes. This article focuses on EAP-based actuator basic properties. Future work will explore how EAP sensors can be integrated into mirror systems.

K. Thetpraphi, Prof. M. Q. Le, Dr. A. Houachtia, Prof. P.-J. Cottinet, Prof. L. Petit, Prof. D. Audigier, Prof. J.-F. Capsal
LGEF (Laboratoire de Génie Electrique et Ferroélectricité), EA682
INSA Lyon (Institut National des Sciences Appliquées)
Université de Lyon
F-69621 Villeurbanne, France
E-mail: jean-fabien.capsal@insa-lyon.fr

Prof. J. Kuhn
Institute for Astronomy
University of Hawaii
34 Ohia Ku St, Pukalani, Maui, HI, USA

Dr. G. Moretto
Centre de Recherche Astrophysique de Lyon (CRAL)
9 avenue Charles André, 69230 Saint-Genis-Laval, France

 The ORCID identification number(s) for the author(s) of this article can be found under <https://doi.org/10.1002/adom.201900210>.

DOI: 10.1002/adom.201900210

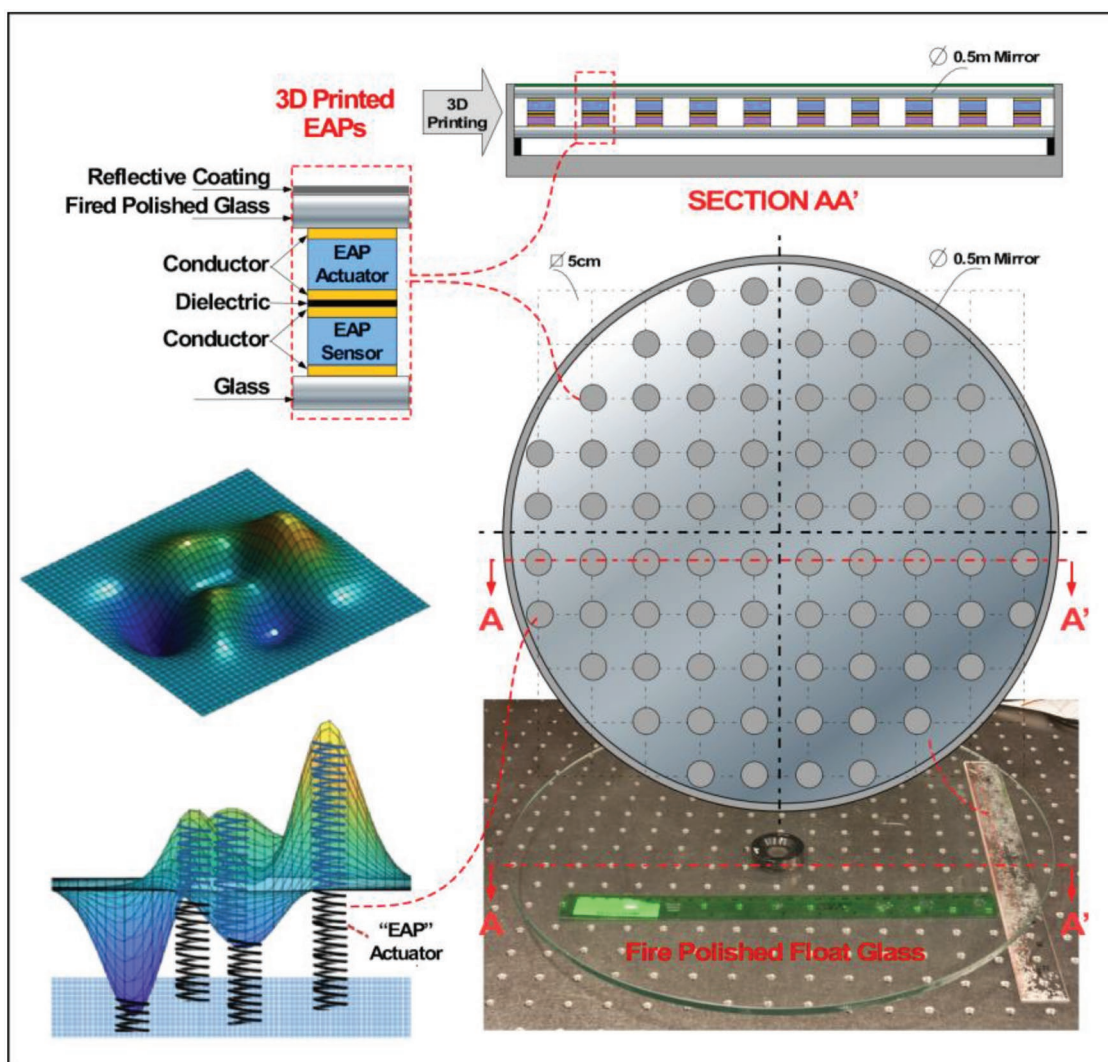


Figure 1. (Left-Bottom): A simulated warpable glass surface and the surface force correction mechanism: the surface roughness is controlled by the electromechanical activity generated in each “EAP-spring” actuator. (Right): A design for the hybrid structure Live-Mirror a sandwich of warpable surfaces separated by a lattice of variable force EAP actuators in series with force EAP sensors. The upper surface (fired polished glass) is called the control surface and the lower surface (glass) is the reaction surface. The static force of each force EAP sensors is controllable and determined by independent metrology of the top surface shape. This particular sensor-actuator geometry assumes preliminarily only vertical (gravity) external force components with assumed lateral material stiffness of the actuators. Section AA’–The 1/2 meter Live-Mirror prototype using the additive manufacturing via 3D Printing technology is in development to fulfill the miniaturized requirements: each individual sensor-actuator system must fit into a circle of less than 5 cm diameter (pitch).

2. Electroactive Polymers Selection

EAPs are currently a most promising class of materials due to their useful properties such as light-weight with high compliance, high active strain and stress, and easy processing to large area films, plus the outstanding capability to be 3D printed into diversified electronic devices such as actuators, generators, sensors, and among others dielectric elastomers.^[7–12] Notably, fluorinated electroactive polymers^[13–15] exhibit exceptional electromechanical response by using different methods such as introducing nanoparticles into polymer matrix,^[16] irradiation approach,^[17] etc., opening exciting opportunities for the future developments of these materials.

Application of EAPs as actuator had been limited due to its lack of ability to provide large deformation and/or force exertion. Promising developments incorporating a plasticizer into an EAP matrix improves radically the its strain response and mechanical energy density.^[18,19] Such a chemical modification leads to large dipolar interfacial effects within the polymer matrix, a contribution of charge trapping between amorphous and crystalline phases, giving rise to increase of dielectric permittivity and simultaneously decrease of Young’s modulus.^[20]

In the case of dielectric polymer, the electrostrictive strain can be generated under electric field attributed to dipolar orientation within the material (Maxwell forces). In the longitudinal

direction, the compressive Maxwell strain S_{33} under a given electric field can be expressed as:

$$S_{33} = M_{33} E_3^2 + s^E T_3 \quad (1)$$

where S_{33} is the longitudinal strain, T is the stress, E is the electric field, M is the electrostrictive coefficient, s is the compliance at E constant. The electrostrictive coefficient term depends on the dielectric permittivity and the Young's modulus of material that can be given by:

$$M_{33} \propto \frac{\epsilon_0 \epsilon_r}{Y} \quad (2)$$

where ϵ_0 and ϵ_r are the vacuum and relative dielectric permittivity, respectively, Y is the Young's modulus of sample. Regarding Equations (1)–(2), the strain can be improved by simultaneously increasing permittivity and reducing Young's modulus. It is possible to apply high electric field but this parameter is however limited by dielectric breakdown strength of material. As reported on,^[19] the figure of merit (FOM) of the strain can be defined by:

$$\text{FOM}_{\text{strain}} = \frac{\epsilon_0 \epsilon_r}{Y} \quad (3)$$

In the longitudinal case when $S_{33} = 0$ yields to stress T_3 :

$$T_3 = Y M_{33} E^2 \quad (4)$$

Combining Equations (2) and (4) makes it possible to induce the FOM of the blocking force for a given electric field

$$\text{FOM}_{\text{force}} = \epsilon_0 \epsilon_r \quad (5)$$

The above Equations (3) and (5) demonstrate that the mechanical strain and the blocking force under low electric field can be simultaneously enhanced by increasing the dielectric permittivity of polymer. For a better electromechanical coupling, especially in low-frequency actuator applications, a decrease of the Young modulus should be involved but it must be limited in order not to drastically change the elasticity or the compliance of the materials.

As it was demonstrated in ref. [13] the P(VDF-TrFE-CFE) terpolymer exhibited significantly higher dielectric constant (i.e., the permittivity) with respect to the conventional EAPs and the PVDF-based copolymer. This makes a terpolymer as one of the most appropriate candidates for various applications in actuator devices where high electromechanical coupling is required. The electrostrictive strain as well as the blocking force of the P(VDF-TrFE-CFE) could be further improved by doping plasticizer molecule into the polymer matrix.^[19] This remarkably simple method showed the possibility to achieve excellent mechanical energy density with around 5.5 times lower in electric field as opposed to the conventional terpolymer.^[14] The results allowed to confirm that terpolymer filled with plasticizer promoted to improve molecular mobility and large Maxwell-Wagner-Sillars interfacial polarization effects at low frequency. These phenomena lead to decrease in Young modulus and increase in dielectric permittivity of the material. As reported in ref. [18]

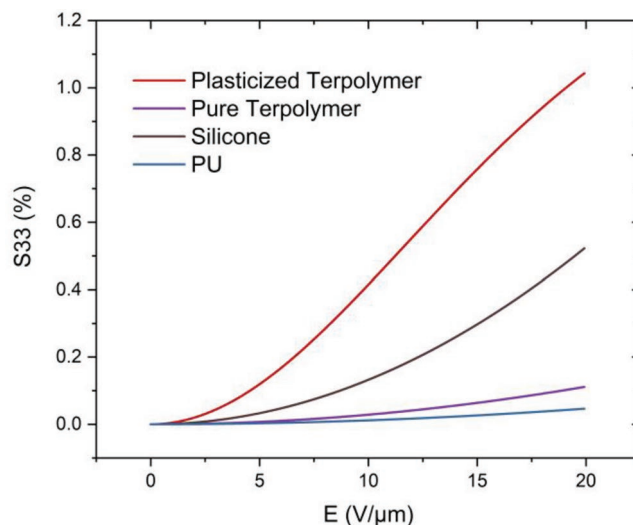


Figure 2. Longitudinal strain without preloading under different applied electric field.

diisononyl phthalate (DINP) plasticizer presents biocompatibility characteristics and best electromechanical response compared to Palamoll 652 and DEHP (2-ethylhexyl phthalate) under the same electric field excitation. Consequently, P(VDF-TrFE-CFE) terpolymer doped with DINP was chosen in this study for achieving high mechanical deformation and driven force.

Figure 2 depicted the free longitudinal strain without preloading (i.e., the stress $T = 0$) versus the applied electric field of four different EAPs, i.e., 1) plasticized terpolymer (terpolymer + 10 wt% DINP), 2) pure terpolymer, 3) silicone, and 4) polyurethane (PU). Such experimental results corroborate the theoretical model of Equation (1) where a quadratic relationship between the strain response and the input electric field was obtained.

Notably the DINP plasticized terpolymer showed an improvement of longitudinal strain (and deformation) as 10 times higher with respect to the neat terpolymer under a moderate $E = 20 \text{ V } \mu\text{m}^{-1}$, and substantially greater than the silicone and the PU under related electric field. Determinatively the DINP plasticizer incorporated into the terpolymer matrix strongly improved the molecular mobility of the amorphous phase,^[14] leading to hugely increased dielectric permittivity under low frequency (50 mHz).

The blocking force is the maximum load that an EAP can generate, i.e., $S = 0$.^[21] **Figure 3** shows the blocking force of the four EAPs (logarithmic scale) versus of the applied electric fields confirming the excellent ability of the plasticized terpolymer to sustain under high load up to 300 N at $E = 20 \text{ V } \mu\text{m}^{-1}$. Bear in mind that the goal blocking force required for active optics controlling-based terpolymer doped with plasticizer (Live-Mirror) is about 1 N for a spatial pitch of one actuator every 5 cm radius.

3. Multilayer Actuator Optimized to Strain Improvement

The optimized EAP modification carries out the increase of dielectric permittivity, low loss rate of energy, improving dielectric

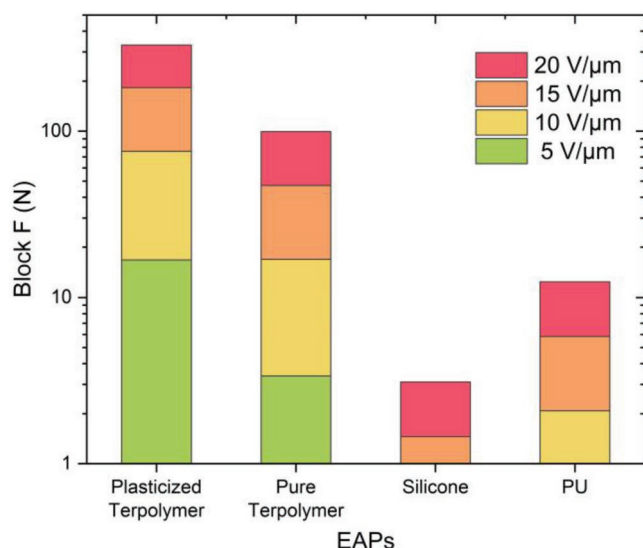


Figure 3. Blocking force (Block F) of different EAPs at different level of electric field.

breakdown strength. Mitigation approach toward dedicated and improved EAPs is the multilayer-actuator-assembly.^[22] Several investigations have been realized in the multilayer topologies for actuator applications in order to achieve a low driven voltage, low dissipation factor, low leakage current, high dielectric breakdown strength, high mechanical response, and high energy density.^[23–26] Multilayer topologically structured demonstrates a number of advantages over conventional materials and other actuator systems. Since a few decades, multilayer piezoelectric actuator manufacturing has been developed in a several applications: bi-stable MEMS switches,^[27] ultrasonic drills and stacked ultrasonic transducers,^[28] and piezoelectric stack actuator for fuel injector.^[29] Recently, polymer plays an important role on smart materials for sensor-actuator applications. Such a high activation field ($\approx 100 \text{ V } \mu\text{m}^{-1}$) is still required to produce large strain for EAP actuator^[30] as well as long-term stability, costs and toxicity, for example, of nanoparticle polymer composites. As a result of scientific difficulty and environmental impact, this leads to many scientific researches carried out EAP multilayer technologies by the significantly rising number of applications. Due to the principle of multilayer actuator,^[25] the popular structure is typically multilayer stack made by connecting EAPs electrically in parallel as a stack of n layers. The particular interest of multilayer stack topologically structured development is its low cost, simple component fabrication (1D assembly), and low voltage supplies needed.^[25] For example, technique layer-by-layer (LbL) assembly of polyethyl- enimine (PEI)/poly(acrylic acid) (PAA) and PU/PAA has been used for a vapor-driven multilayer polymer actuator.^[31] Film capacitor fabricated through LbL of PVDF/P(VDF-TrFE-CTFE)/PVDF composites was able to reach dielectric constant of 18.61 with a sandwich-structure.^[32] DEAP-based multilayer stack-actuators have been developed for a novel automated actuator manufacturing process to maximize the force or absolute deformation.^[24]

In this study, stack multilayer design was investigated in order to achieve an EAP with extremely enhanced permittivity,

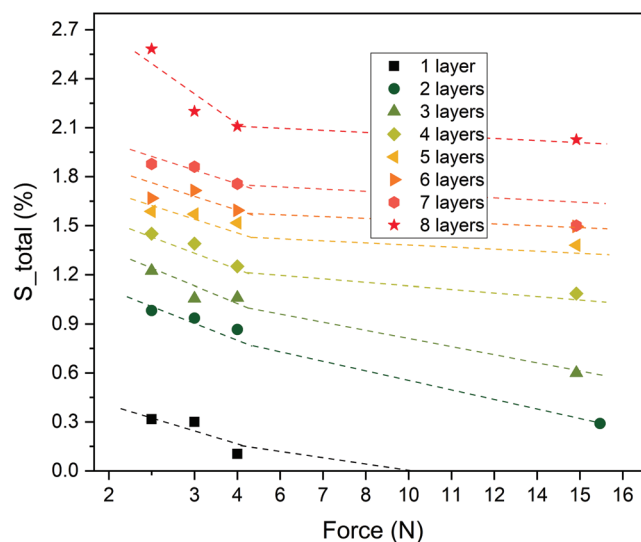


Figure 4. Total strain S generated by multilayer plasticized terpolymer under an external applied force F .

low losses, and high displacement/load at somewhat low driving voltages. Considering the force-served actuator, we assess the electrostrictive performance of the plasticized terpolymer in function to the layer numbers n . The multilayers films were modeled as a structure of capacitors in parallel mode (electric connection for each single film layer) stack, e.g., its capacitance increase directly proportional to the n number of layers.

Figure 4 shows the total strain in terms of force (i.e., deduced from additional weight) for $n = 1, \dots, 8$ layers stack. Different weights simulating the external preloading from 250 to 1500 g were directly applied on the active area of the multilayer samples. Longitudinal strain gradually decreased versus the applied force at $E = 10 \text{ V } \mu\text{m}^{-1}$. Interestingly, when the applied force reached 15 N, the total strain was still different from zero, reflecting excellent actuation performance of the plasticized multilayer terpolymer under high load condition. Wrapping up the exerted force to doped terpolymer is still far from the presented blocking force in **Figure 3**. The multilayer actuator capability of plasticized terpolymer undoubtedly showed substantial improved strain response stimulated by low input excitation and showed the possibility to accomplish correction of the Live-Mirror (**Figure 1**) goal average strain/displacement in gravity direction correction in a few microns.

4. Trial Glass Surface Deformation with One Actuator Stack

In order to validate the actuator proof-of-concept for controlling glass surface shape deformation, the plasticized terpolymer (with $n = 8$ -layer stack) was integrated between two sheets ($15 \times 15 \text{ cm}$) of flat glass 3 mm thick, settled in parallel and clamped with two aluminum support and four inactive spacers (**Figure 5**).

Figure 5 shows the results for the quasi-static displacement versus position of the glass under low electric fields of

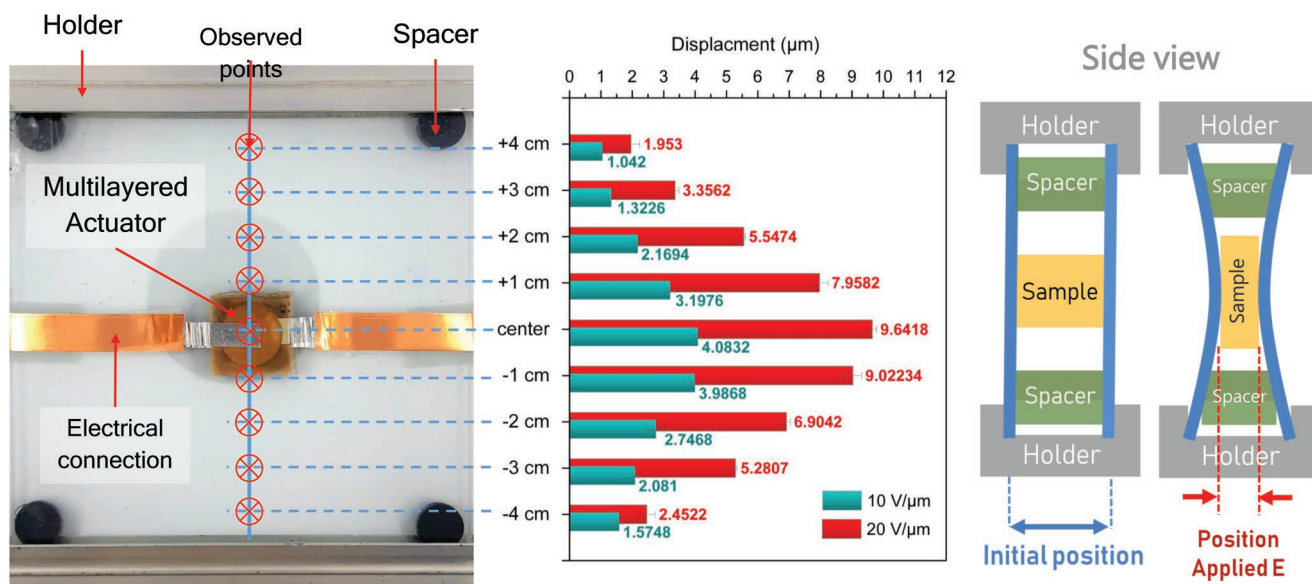


Figure 5. The proof of one actuator multilayer stack inserted between two plates of glass and the corresponding displacement in different positions at applied electric field of 10 and 20 V μm^{-1} .

10 and 20 V μm^{-1} . The glass surface deformation attained the maximum value at the center position (actuated area), and gradually decreased when farther from actuated area. The measurement of the glass surface deformation has been done via a noncontact laser displacement sensor.^[33] One could ask why the slightly asymmetric behavior of the displacement plots. It is due to the fact that the holder clamp forces on the glass surface were not perfectly identical. In the end, the proposed device can achieve a deformation of 10 μm with sufficient driven force. Deformation value fulfills the requirement of actuation performance in shaping the Live-Mirror (Figure 1) goal displacement in vertical direction correction in a few microns.

5. Results

A longitudinal multilayer force-actuator stack on glass has been validated in the lab. **Figure 6A** shows an actuator stack of plasticized terpolymer sandwiched between two commercial flat circular glass plates that form a front mirror surface (the 'control' surface, Sc) and a reaction surface (Sr). Both plates are 110 mm in diameter and 3 mm thick. **Figure 6A** shows how the parallel plates are glued together with three 0.7 mm diameter \approx 2 mm thick cylindrical inactive spacers arranged in a triangle of side length 50 mm centered on the actuator stack. The spacers are slightly thinner than the actuators so that the stack experiences

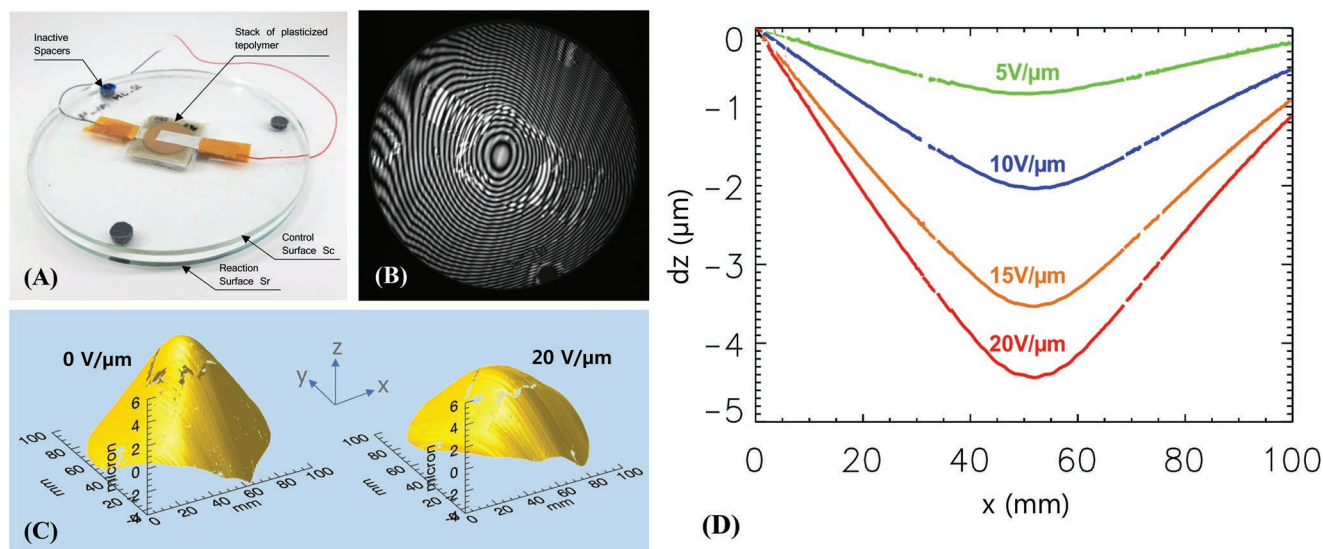


Figure 6. A) An 8-layer stack of plasticized terpolymer sandwiched between two flat circular glass plates: reaction surface (Sr) and control surface (Sc). B) The interferometer intensity fringes ($E = 0 \text{ V } \mu\text{m}^{-1}$) from the front glass control surface (Sc). C) The 3D-surface for the control surface (Sc) at $E = 0$ and $20 \text{ V } \mu\text{m}^{-1}$ is derived from interferometer fringes (B). D) The change of the front control surface (Sc) along a horizontal cut through the glass bump under different applied electric fields. All measurements were done with a Fizeau laser (633 nm) interferometer (Zygo verifire).

a “preload” compression force of a few newtons per square centimeter. Figure 6B shows the surface (Sc) shape deformation intensity fringes for $E_0 = 0 \text{ V } \mu\text{m}^{-1}$. Figure 6C shows the 3D shape of the front surface glass bump from the preload at two different actuator voltages. The change in the front sheet glass surface shape with actuator voltage is apparent. The deformation was quantitatively obtained from the difference of the interferometrically measured front control surface for an applied electric field ranging from $E_0 = 0 \text{ V } \mu\text{m}^{-1}$ to $E_{20} = 20 \text{ V } \mu\text{m}^{-1}$.

Figure 6D shows this shape change along a horizontal line centered on the actuator after subtracting the shape at zero electric field. The difference of the displacement (dz) in the z -direction versus the x -position along the diameter of the control surface of glass is plotted here where the negative sign of dz signifies a contraction of the glass sandwich in the z -direction.

As expected, the magnitude of dz increased with the input voltage excitation with a maximum value at the location of the center of the actuator. Also, the glass deformation amplitude (dz) increases faster than linearly with field strength (c.f. Figure 2) as expected for the electrostrictive effect. We note that the sample will expand in the transversal direction as the longitudinal actuator shrinks where the actuator stack is glued to the glass. This shear force is ignored here but will be considered and modeled in further actuator assessments.

Our proof-of-concept actuator multilayer stack creates a controllable contraction in the z -direction when it is sandwiched between glass surfaces. The overall glass separation deformation, accounting for both surfaces, is about 10 microns for conventional high voltage drivers. Since EAP actuators are relatively inexpensive and can, in principle, be created on glass using typical additive manufacturing methods, we believe this technique is promising for the development of precise large active mirror surfaces.

6. Conclusion

This work shows the feasibility of electroactive polymers for active optics applications using doped terpolymer. In addition, our multilayer stack-actuator assembly yielded a sufficiently large strain response to shape optical glass mirrors with shape changes of several microns and large deformation forces. We have demonstrated the possibility of large strain displacements together with significant blocking forces in multilayer EAP actuators. This opens the door to different scientific investigations—for example in hybrid dynamic structures for optical quality surface shape control.

We expect to fabricate these light-weight mirrors as a hybrid material composed of two layers of millimeter-scale thick glass and two layers of electroactive material with a final very light mechanical truss. In the particular case of an optical telescope for astronomy^[3,4,6] a printable 200 micron scale thick layers of plasticized terpolymer—as demonstrated here—can have an area energy density sufficient to bend millimeter-scale thick glass by several microns. These mirrors would not be abrasively polished; the first EAP layer essentially ‘polishes’ the centimeter-scale nonuniformities in the reflecting surface (acting from the back side) of commercial fire-polished glass using shear stress. In our hybrid a second glass sandwich layer (Figure 6) provides a force reaction surface and an electrostatically stiff paraboloidal shape. Printed, large-strain stacked force-controlled actuators

acting between the reaction surface and the mirror surface will tolerate a distorted reaction surface. Thus a few millimeters thick reaction surface, stiffened by printed shear actuators, could be supported by a very light mechanical truss while it accommodates the strain range of the mirror-surface actuators. The total moving mass density of a telescope based on these optics could be in the order of 200 kg m^{-2} or less. The overall effect of this 1 cm thick active hybrid mirror structure is to electronically create $100\times$ more stiffness than a conventional and massive thick mirror. Currently planned massively segmented telescopes like the European Extremely Large Telescope^[2] or the Thirty Meter Telescope,^[34] use “Keck-era”^[35] optics. Their mirror subapertures create a dynamically rigid primary optical surface from 100s of 1 m scale few centimeters thick mirrors. The potential for building the next generation of extremely large telescopes increases with the ability to decrease the mirror mass density since this payload mass sets the cost scale for the entire optomechanical structure.

In the future we want to use hybrid and multilayer doped terpolymers to make smart remote sensing systems. This pushes development toward optimized and miniaturized EAP actuator-sensors. For instance, with 3D-printed terpolymers with flexible electrodes on the back of a mirror, many-actuator degree-of-freedom optical elements will be possible. The ultimate goal is to demonstrate a novel hybrid “smart” metamaterial with superior stiffness-to-density ratio mechanical properties for general optical applications.

Acknowledgements

This work was supported by **Live-Mirror** project funded by ANR (The French National Research Agency): Project #ANR-18-CE42-0007-01 and by DPST jointly administered by the ministry of education and the Institute for the promotion of teaching science and technology Thailand, Franco-Thai scholarship 2016 from Campus France. The authors are grateful to INSA-Lyon visiting professor program supporting Prof. J.R. Kuhn and also to the collaborators and members of PLANETS Foundation (<https://www.planets.life>).

Conflict of Interest

The authors declare no conflict of interest.

Keywords

electroactive polymers, low-scattered light mirror, multilayer actuators, optical surface correction, plasticized doped terpolymers, surface shape control

Received: February 1, 2019

Revised: March 20, 2019

Published online:

[1] H. Henniger, O. Wilfert, *Radioengineering* **2010**, *19*, 203.

[2] European Southern Observatory, The European Extremely Large Telescope, <https://www.eso.org/public/teles-instr/elt/> (accessed: March 2019).

- [3] J. R. Kuhn, G. Moretto, R. Racine, F. Roddier, R. Coulter, *Publ. Astron. Soc. Pac.* **2001**, *113*, 1486.
- [4] G. Moretto, J. R. Kuhn, J. F. Capsal, D. Audigier, K. Thetraphi, M. Langlois, M. Tallon, M. Gedig, S. V. Berdyugina, D. Halliday, presented at *Ground-based and Airborne Telescopes VII*, Austin, TX, July **2018**, *Proceedings of SPIE Vol. 10700*, <https://doi.org/10.1117/12.2312599>.
- [5] G. Moretto, J. R. Kuhn, S. Berdyugina, M. Langlois, M. Tallon, E. Thiébaud, D. Halliday, presented at *Ground-based and Airborne Telescopes VI*, Edinburgh, UK, August **2016**, *Proceedings of SPIE Vol. 9906*.
- [6] J. R. Kuhn, S. V. Berdyugina, M. Gedig, M. Langlois, G. Moretto, K. Thetraphi, presented at *Ground-based and Airborne Telescopes VII*, Austin, TX, July **2018**, *Proceedings of SPIE Vol. 10700*.
- [7] F. Bauer, *IEEE Trans. Dielectr. Electr. Insul.* **2010**, *17*, 1106.
- [8] L. Yang, X. Li, E. Allahyarov, P. L. Taylor, Q. M. Zhang, L. Zhu, *Polymer (UK)* **2013**, *54*, 1709.
- [9] F. Bauer, E. Fousson, Q. Zhang, *IEEE Trans. Dielectr. Electr. Insul.* **2006**, *13*, 1149.
- [10] A. O'Halloran, F. O'Malley, P. McHugh, *J. Appl. Phys.* **2008**, *104*, 071101.
- [11] J. Biggs, K. Danielmeier, J. Hitzbleck, J. Krause, T. Kridl, S. Nowak, E. Orselli, X. Quan, D. Schapeler, W. Sutherland, J. Wagner, *Angew. Chem., Int. Ed.* **2013**, *52*, 9409.
- [12] F. Pedroli, A. Marrani, M. Q. Le, C. Froidefond, P. J. Cottinet, J. F. Capsal, *J. Polym. Sci., Part B: Polym. Phys.* **2018**, *56*, 1164.
- [13] Prateek, V. K. Thakur, R. K. Gupta, *Chem. Rev.* **2016**, *116*, 4260.
- [14] J. F. Capsal, J. Galineau, M. Lallart, P. J. Cottinet, D. Guyomar, *Sens. Actuators A* **2014**, *207*, 25.
- [15] F. Li, L. Jin, Z. Xu, S. Zhang, *Appl. Phys. Rev.* **2014**, *1*, 011103.
- [16] Z.-M. Dang, J.-K. Yuan, S.-H. Yao, R.-J. Liao, *Adv. Mater.* **2013**, *25*, 6334.
- [17] L. Yang, X. Li, E. Allahyarov, P. L. Taylor, Q. M. Zhang, L. Zhu, *Polymer* **2013**, *54*, 1709.
- [18] N. Della Schiava, M. Q. Le, J. Galineau, F. Domingues Dos Santos, P. J. Cottinet, J. F. Capsal, *J. Polym. Sci., Part B: Polym. Phys.* **2017**, *55*, 355.
- [19] N. Della Schiava, K. Thetraphi, M. Q. Le, P. Lermusiaux, A. Millon, J. F. Capsal, P. J. Cottinet, *Polymers* **2018**, *10*, 263.
- [20] J.-F. Capsal, M. Lallart, J. Galineau, P.-J. Cottinet, G. Sebald, D. Guyomar, *J. Phys. D: Appl. Phys.* **2012**, *45*, 205401.
- [21] Forces and Stiffness, <https://www.piceramic.com/en/piezo-technology/properties-piezo-actuators/forces-stiffnesses/> (accessed: December 2018).
- [22] E. Baer, L. Zhu, *Macromolecules* **2017**, *50*, 2239.
- [23] Z. Zhou, M. Mackey, J. Carr, L. Zhu, L. Flandin, E. Baer, *J. Polym. Sci., Part B: Polym. Phys.* **2012**, *50*, 993.
- [24] J. Maas, D. Tepel, T. Hoffstadt, *Meccanica* **2015**, *50*, 2839.
- [25] J. Pritchard, C. R. Bowen, F. Lowrie, *Br. Ceram. Trans.* **2001**, *100*, 265.
- [26] Y. Wang, J. Chen, Y. Li, Y. Niu, Q. Wang, H. Wang, *J. Mater. Chem. A* **2019**, *7*, 2965.
- [27] M. Dorfmeister, B. Kössl, M. Schneider, U. Schmid, *Proceedings* **2019**, *2*, 912, <https://doi.org/10.3390/proceedings2130912>.
- [28] D. J. Powell, G. Hayward, S. Member, R. Y. Ting, *IEEE Trans. Ultrason. Ferroelectr. Freq. Control* **1998**, *45*, 667.
- [29] M. S. S. Enousy, D. M. Umford, M. G. Adala, R. K. N. D. Rajapakse, *J. Intell. Mater. Syst. Struct.* **2009**, *20*, <https://doi.org/10.1177/1045389X08095030>.
- [30] Y. Bar-Cohen, Q. Zhang, *MRS Bull.* **2008**, *33*, 173.
- [31] Y. Song, S. Qin, J. Geringer, J. Grunlan, *Soft Matter* **2019**, *15*, 2311.
- [32] L. Wang, H. Luo, X. Zhou, X. Yuan, K. Zhou, D. Zhang, *Composites, Part A* **2019**, *117*, 369.
- [33] The Microtrak II CMOS laser triangulation technology for precise measurements of displacement, position, vibration and thickness.
- [34] TMT International Observatory, Thirty Meter Telescope Astronomy's Next-Generation Observatory, <https://www.tmt.org/> (accessed: March 2019).
- [35] W. M. Keck Observatory, Keck I and Keck II Telescopes, <http://www.keckobservatory.org> (accessed: March 2019).